Supplementary material

Engineering thermally activated $NiMoO_4$ nanoflowers and biowaste derived activated carbon-based electrodes for high-performance supercapatteries

C. Justin Raj[a], Ramu Manikandan[b], Kook Hyun Yu[a], Goli Nagaraju[c, d], Myung-Soo Park[e], Dong-Won Kim[e], Sang Yeup Park[f], Byung Chul Kim[b]*

[a] *Department of Chemistry, Dongguk University, Jung-gu, Seoul-04620, Republic of Korea.*

[b] *Department of Printed Electronics Engineering, Sunchon National University, 255, Jungang-ro, Suncheon-si, Jellanamdo 57922, Republic of Korea.*

[c] *Department of Chemical Engineering, College of Engineering, Kyung Hee University, 1732 Deogyeong-daero, Gihung-gu, Yongin-si, Gyeonggi-do 44670, Republic of Korea.*

[d] *School of Chemistry, Trinity College Dublin, Dublin2, Ireland.*

[e] *Department of Chemical Engineering, Hanyang University, Seungdong-gu, Seoul-04763, Republic of Korea.*

[f] *Department of Ceramic Engineering, Gangneung-Wonju National University, Gangneung-25457, Republic of Korea.*

* Corresponding author, E-mail: bckim@scnu.ac.kr (B.C. Kim)

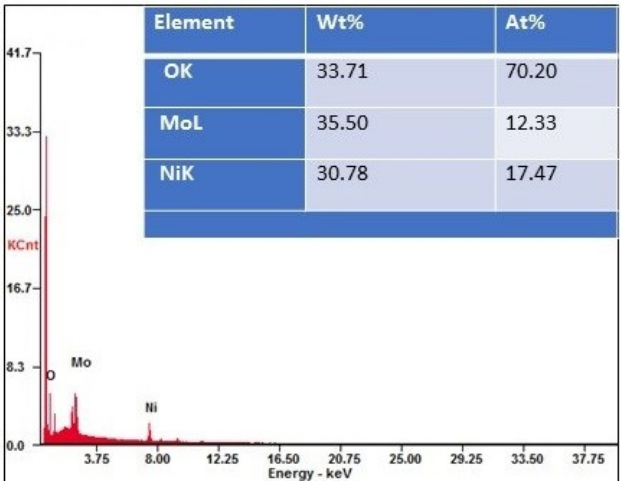

Fig. S1. EDX spectrum of NMO-500 samples and inset table shows the wt.% and At.% of elements exist in the scanned area of the sample.

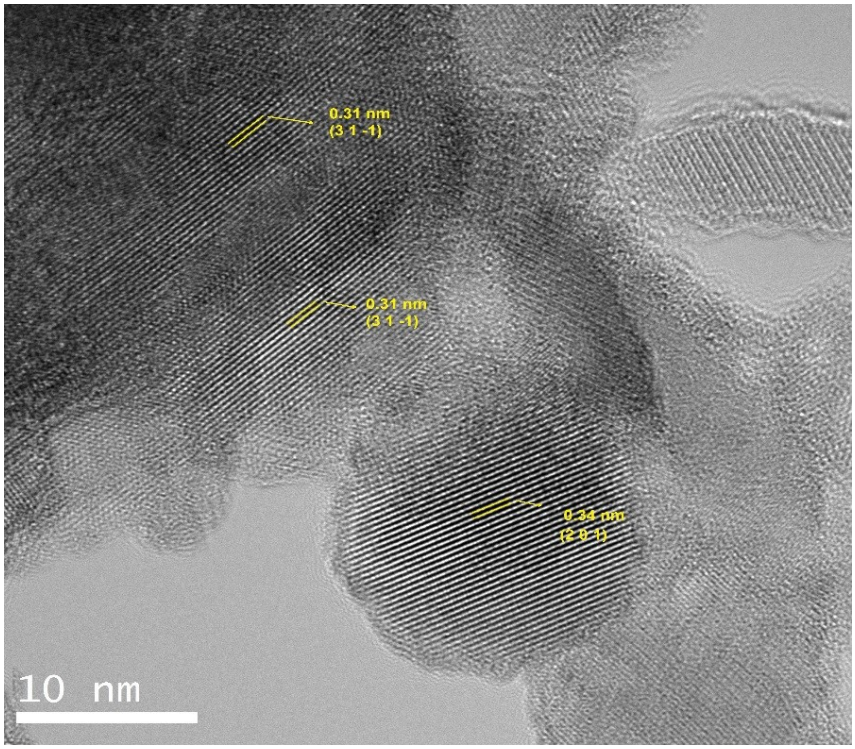

Fig. S2. HRTEM image of NMO-500 samples

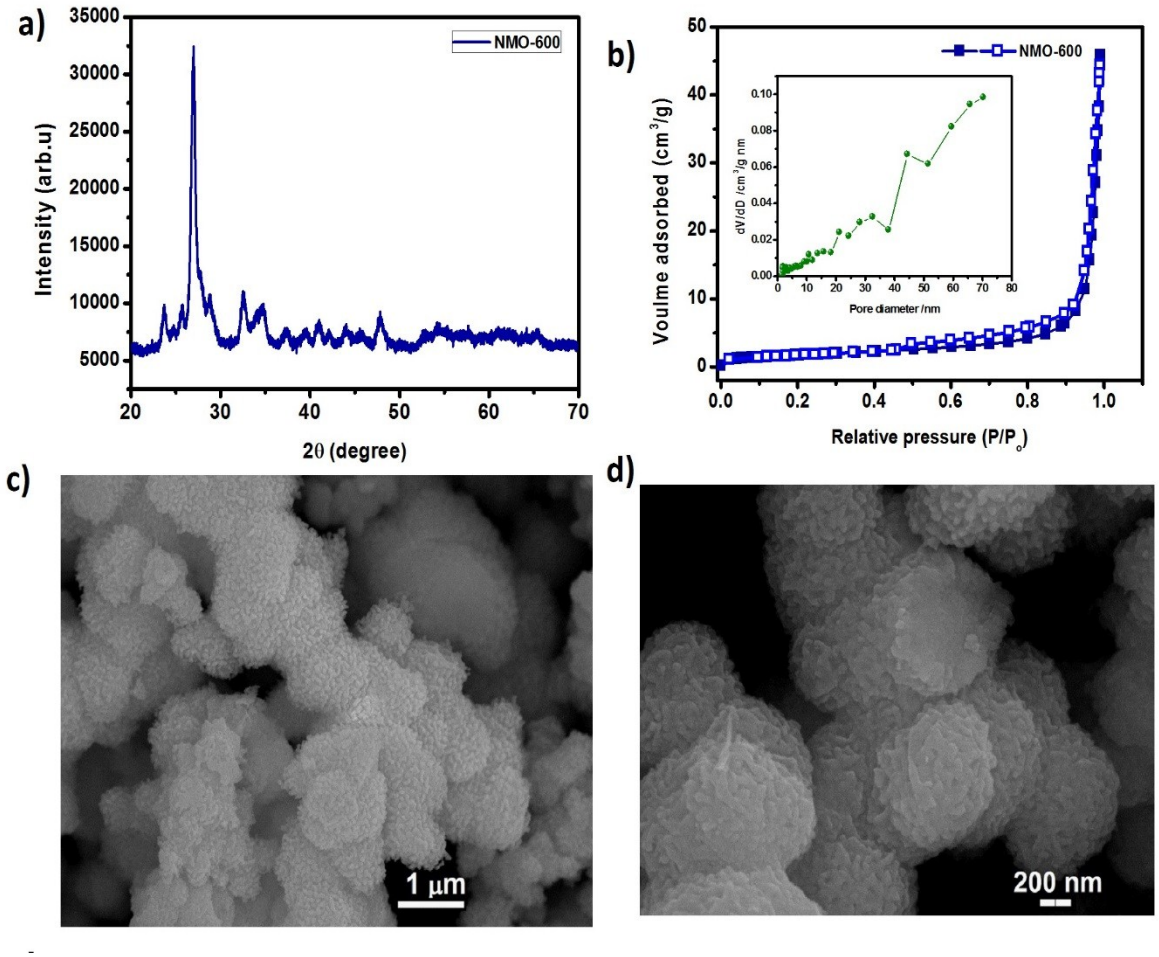

Fig. S3. a) XRD pattern of NMO-600 sample showing good crystalline nature of the sample, b) N_2 adsorption/desorption isotherms of the NMO-600 and the inset shows the pore size distribution of the sample, c) and d) the low and high magnification SEM images of NMO-600 sample.

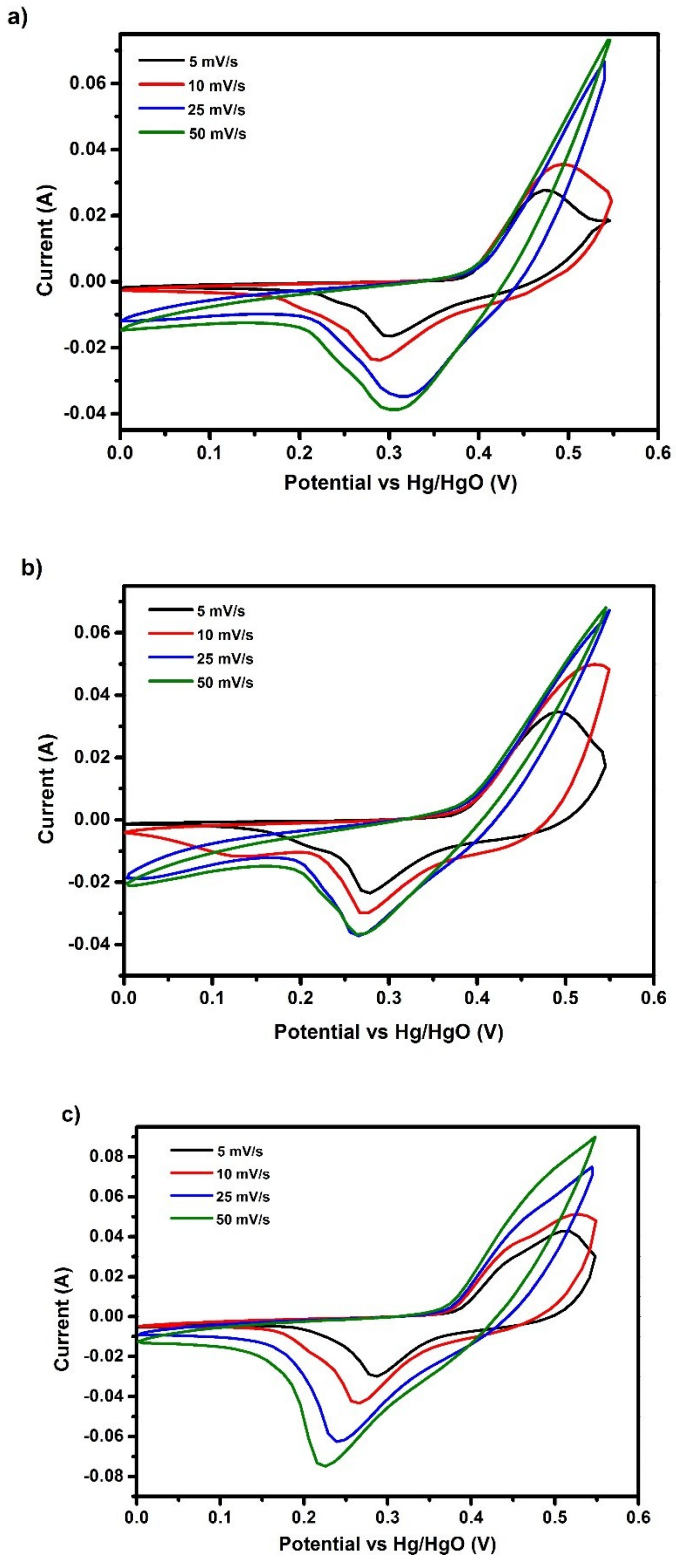

Fig. S4. CVs of the NMO-bare, NMO-400 and NMO-500 electrodes in 6M KOH

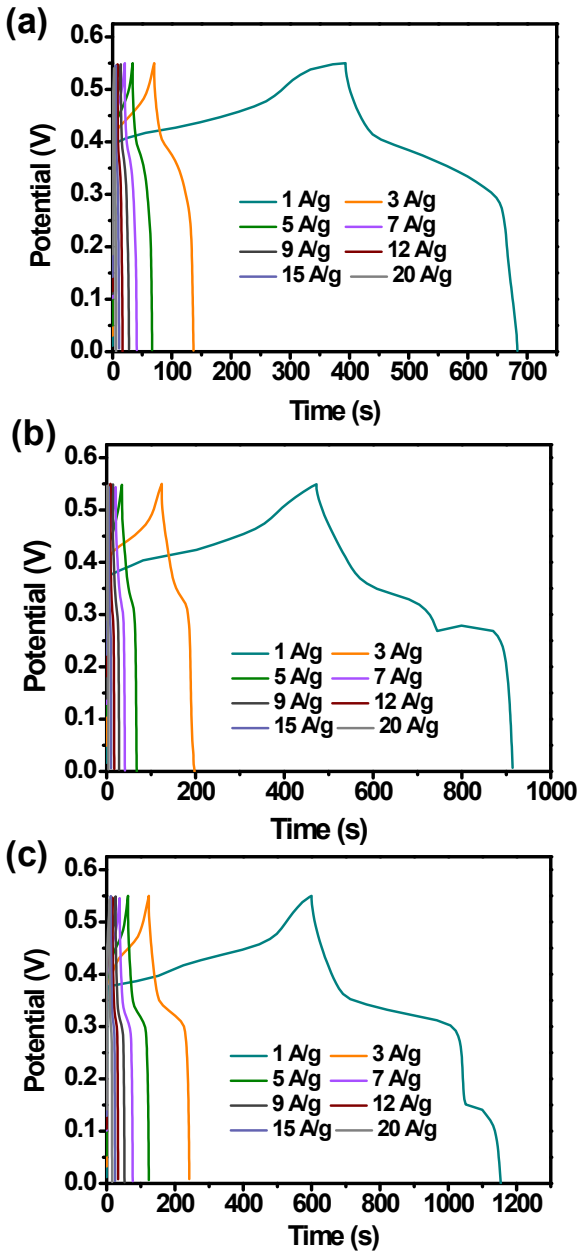

Fig. S5. Charge/discharge curves of the NMO-bare, NMO-400 and NMO-500 electrodes in 6M KOH

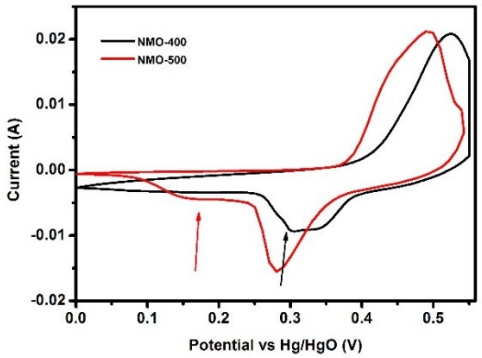

Fig. S6. CVs of the NMO-400 and NMO-500 electrodes at scan rate 2 mVs^{-1}

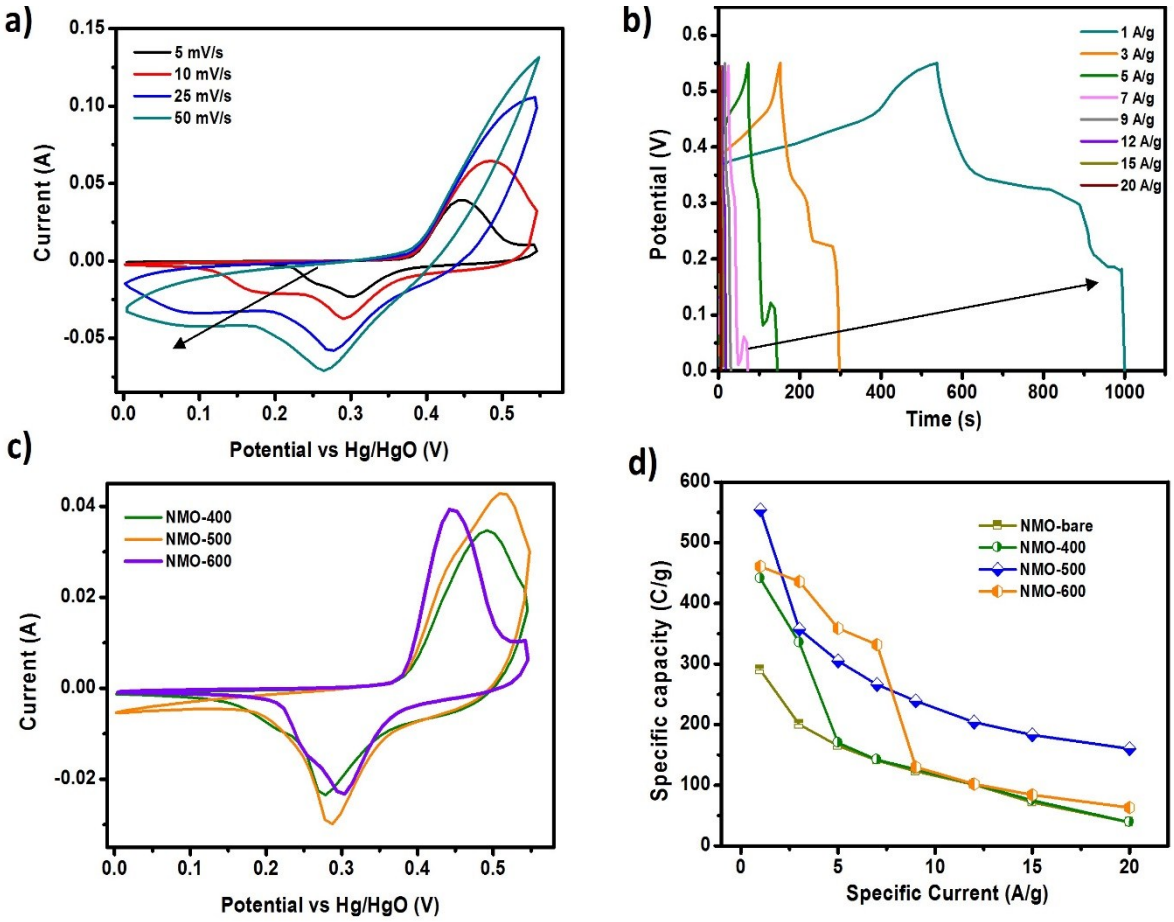

Fig. S7. a) CVs of the NMO-600 electrode in 6M KOH for various scan rates highlighting the secondary reduction peak, b) Charge/discharge curves of the NMO-600 electrode for different specific currents highlighting the discharge plateau, c) CVs of the NMO-400, NMO-500 and NMO-600 electrodes, d) comparison of the specific capacity variation of the NMO-bare, NMO-400, NMO-500 and NMO-600 electrodes.

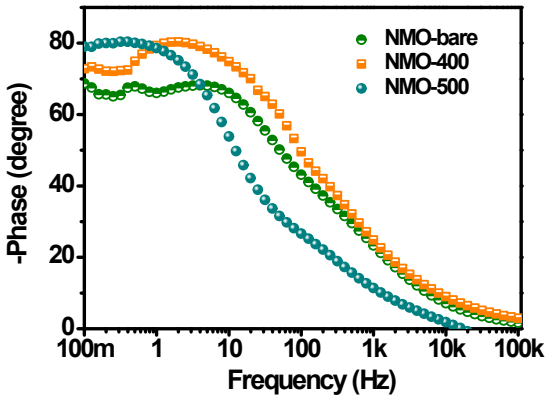

Fig. S8. Bode plots of NMO-bare, NMO-400 and NMO-500 electrodes

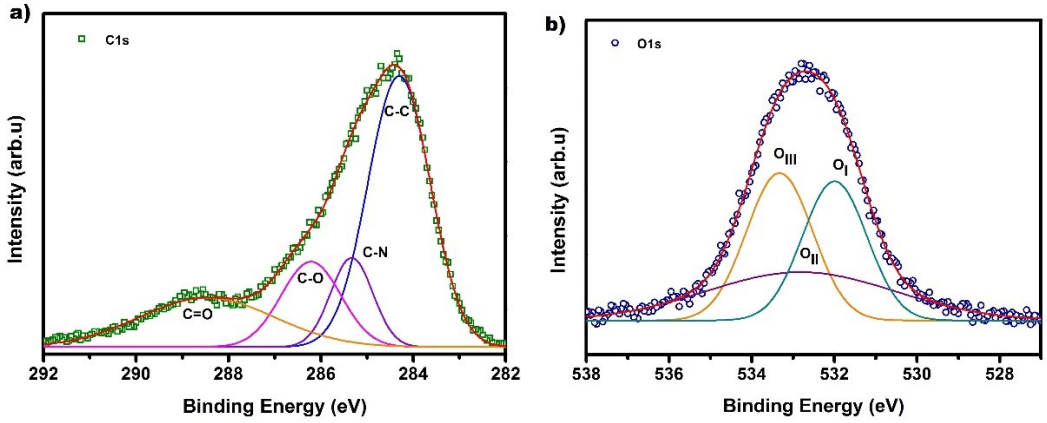

Fig. S9. a) The magnified C1s XPS spectrum of O,N-AC sample, the four peaks at 284.3, 285.3, 286.2 and 288.5 eV represents the C-C, C-N, C-O and C=O groups present in the sample; b) The magnified O1s spectrum of O,N-AC sample, the peaks O_I (531.9 eV), O_{II} (532.8 eV) and O_{III} (533.3 eV) corresponds to the O=C quinine type group, C-O-H Phenol or C-O-C ester group and chemisorbed oxygen or water molecules bonded to the carbon atoms

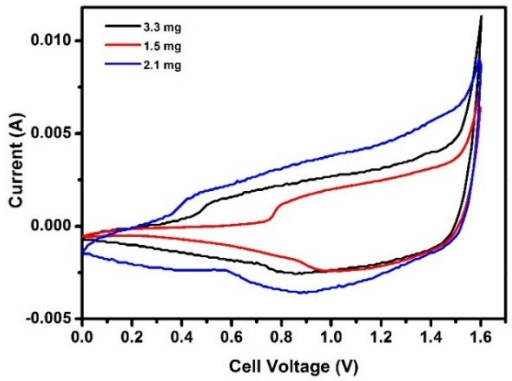

Fig. S10. CVs of the supercapatteries at scan rate 5 mVs^{-1} for various mass of active material in the positive electrode; the negative electrode mass was fixed (~2 mg).

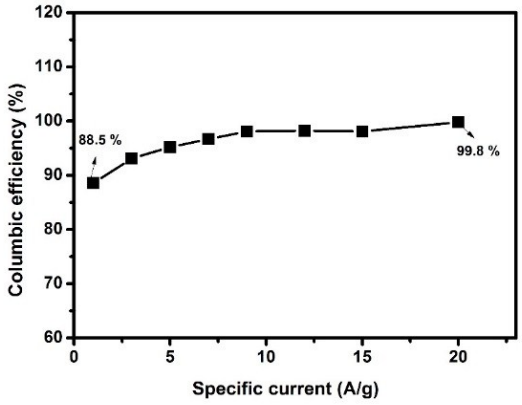

Fig. S11. Variation of columbic efficiency of the supercapattery with various specific currents.